CONTRACT SERIAL NO. 09269-01-SQ
CONTRACTOR: UNIV. OF WESTERN ONTARIO
CONTRACT REQUISITION NO. 23440-0-9269

A Fundamental Study of the Atmospheric Oxidation of Magnesium and Magnesium Alloys

FINAL Report

Cleared for Sonja Harris March 3/92 -sp

By

S.J. Splinter and N.S. McIntyre
Surface Science Western
The University of Western Ontario
London, Ontario
N6A 5B7

For

Canada Centre for Mineral and Energy Technology
568 Booth Street
Ottawa, Ontario
K1A 0G1

16pp

December 1991

MICROMEDIA

92-03694/

SUMMARY

Oxidation processes are being studied on polycrystalline pure magnesium surfaces and on magnesium alloys containing low concentrations of iron. The growth of oxide is monitored on the faces of several grains having different crystallographic orientations. The microscopic analysis is carried out by a scanning Auger microprobe, which is capable of detecting oxide concentrations of < 0.1 of a monolayer using the metallic $Mg(L_{23}VV)$ line, the oxidized $Mg(L_{23})O(L_{23})O(L_{23})$ line and the oxygen $(K_1L_{23}L_{23})$ line. Clean surfaces are prepared by using a minimum dose of argon ions to avoid the creation of heavily disordered crystal planes. By using calibrated doses of D_2O vapour, three stages of early oxidation growth are recognized: a chemisorption stage during doses up to about 0.75 Langmuirs; a rapid oxide nucleation and island growth stage which is complete by about 5 Langmuirs and a slow growth stage after coalescence of the oxide islands. On magnesium alloys containing iron at concentrations ranging from 70 to 700 ppm, the growth rate of the initial oxide is retarded on some grain orientations, with the retardation effect a clear function of iron concentration.

INTRODUCTION

The oxidation of a metal surface has dramatic effects on its bulk properties. The oxide film resulting may impart a chemical stability that maintains desirable mechanical and electrical properties of the bulk. Alternatively, unstable surface oxides can result in internal oxidation and a loss of mechanical and chemical stability.

The oxidation behaviour of magnesium alloys is of particular interest in view of their increasing use in structural applications where light weight is important (e.g. aerospace industries). Oxidation of pure magnesium surfaces has previously been reported by several groups[1-5] using various surface analytical techniques. However, no fundamental studies of any magnesium alloys have been conducted largely because of patent difficulties in preparing fairly large single crystal surfaces ($> 500\mu m^2$) capable of being studied by macroscopic techniques such as low energy electron diffraction (LEED), X-ray photo-electron spectroscopy (XPS) and accelerator-based methods.

The aim of the present research has been to determine the effect that minor alloying elements such as iron and manganese have on the initial oxidation behaviour of magnesium surfaces. Minor additions of such elements have been shown to affect the thickness and nature of the native oxide films formed on magnesium at 25°C and at 100°C in air.[6]

This group has adopted an approach which studies the surface compositions of individual microscopic grain faces found on polycrystalline alloys. Scanning Auger microscopy (SAM) analysis of individual grain faces having widely differing crystallographic orientations is carried out. Initial studies have concentrated on following the early stages of oxide growth on clean (Ar^+ sputtered) surfaces of high-purity magnesium and magnesium-iron alloys containing from 70 to 700 ppm iron using controlled doses of deuterated water vapour.

EXPERIMENTAL

The samples were mechanically polished to a 0.3μm Al_2O_3 finish and cleaned ultrasonically before mounting in a Perkin-Elmer PHI-600 scanning Auger microprobe (base pressure ≅ 10^{-9} Torr). Auger spectra of the specimen surfaces as mounted showed the presence of carbon and oxygen as the principle contaminants (Figure 1(a)). After sputtering with a brief dose of 3 keV argon ions, the Auger spectra revealed only the presence of metallic magnesium (Figure 1(b)).

The clean surfaces were then exposed to calibrated doses of D_2O at 25°C ranging from 0.1 to 100 Langmuirs (L) (1L = 1 x 10^{-6} Torr·second). Several grain faces were chosen for detailed study on the basis of widely differing contrast in their secondary electron channeling images. Auger spectra were obtained using a 3 keV electron beam energy and electron currents ≤ 30nA to minimize electron beam effects. The uptake of oxygen on the clean surfaces was thus monitored *in situ* using the intensity of the metallic $Mg(L_{23}VV)$, the oxidized $Mg(L_{23})O(L_{23})O(L_{23})$ and the $O(K_1L_{23}L_{23})$ Auger lines. The low kinetic energy of the $Mg(L_{23}VV)$ line (45 eV) allows oxide layers ≥ 0.1 monolayer to be detected.

RESULTS AND DISCUSSION

The growth of oxide on one particular orientation of pure magnesium is illustrated in Figure 2(a) where the O(KLL) AES peak-to-peak intensity, normalized to the intensity at saturation, is plotted versus exposure to D_2O. This particular orientation showed bright secondary electron contrast and is shown as grain A in Figure 2(c). The growth of oxide on a grain of substantially different orientation as determined by its contrast (grain B in Figure 2(c)) is shown in Figure 2(b). It is evident that the uptake of oxygen was substantially slower on the grain face exhibiting dark contrast. The vertical error bars in Figure 2 represent the standard deviation calculated from five separate experiments.

The study of oxide growth kinetics on the series of iron alloys has revealed that, on grains showing bright contrast, the rate is substantially influenced by the concentration of iron present. This is illustrated in Figure 3(a) where the data have been fitted to a two-dimensional nucleation and growth model.[7] The slope of the straight lines in Figure 3 represents the rate of oxygen uptake on clean surfaces. It is clear that alloying pure magnesium with increasing levels of Fe ranging from 70 ppm to 700 ppm leads to a progressive decrease in the rate of oxide film growth. Interestingly, the same effect was not observed for grains exhibiting dark contrast (see Figure 3(b)).. Nevertheless, this is the first known example where the presence of a very minor constituent has been shown to alter the oxide growth rate from the earliest possible stage. The mechanism for this effect is not yet understood, but it may result from a decrease of lateral mobility of oxygen atoms caused by iron sites.

The growth of oxide after much higher exposures has also been followed. Figure 4 shows the changes in the low-energy magnesium Auger signal for increasing exposures of D_2O on a grain of pure magnesium exhibiting dark secondary electron channeling contrast. The 45 eV signal represents the main metallic $Mg(L_{23}VV)$ transition, the 34 eV signal represents the main oxide $Mg(L_{23})O(L_{23})O(L_{23})$ transition and the 27 eV signal represents an interfacial $Mg(L_{23})O(L_{23})Mg(V)$ transition.[4] From Figure 4 it is evident that increasing exposures to D_2O leads to an attenuation of the metallic Mg signal and a growth of the oxidized Mg signal. In addition, the presence of an interfacial transition at exposures as low as 0.5L indicates that there is true chemical bonding between the oxygen present on the surface and the magnesium substrate. In other words, it is apparent that the initial interaction of D_2O with magnesium results in a chemisorptive rather than a physisorptive process.

The kinetics of the oxidation process can be determined by carefully monitoring the attenuation of the metallic 45 eV Auger line intensity. In Figure 5(a), the AES peak-to-peak intensity of

the Mg($L_{23}VV$) transition, I_{Mg}, normalized to the clean magnesium signal, I^{∞}_{Mg}, is shown for increasing exposures to D_2O. An estimation of an equivalent relative oxide film thickness is easily obtained, assuming that the metal is covered with a uniform, homogeneous oxide layer. Although this is not exactly the case, as shall be discussed, useful information can be obtained on the amount of oxidized magnesium and its growth kinetics.

For an homogeneous film of thickness d covering the surface, the signal intensity is given by:

$$I_{Mg} = I^{\infty}_{Mg} \cdot \exp(-d/\lambda) \qquad (1)$$

where λ is the escape depth of the measured (45 eV) electrons. Equation (1) has been used with the I_{Mg}/I^{∞}_{Mg} data of Figure 5(a) to calculate the relative film thickness, d/λ, and the results are shown in Figure 5(b). From Figure 5(b) it is evident that there are three distinct regions of oxygen uptake on magnesium: slow uptake until about 0.75 L exposure; a rapid increase in uptake rate between about 0.75 L and about 5 L; and a slower, more gradual increase to higher exposures. This behaviour has been observed for other metals[8-10] and has been interpreted as being due to the following general sequence of the oxidation process: (i) chemisorption; (ii) oxide nucleation and growth by islands until coalescence; and (iii) thickening of the oxide film by transport of the reactive species through the oxide film.

Equations (2) and (3) describe the kinetics of the first two stages of the oxidation respectively:[9-11]

$$I_{Mg}=I^{\infty}_{Mg}\left[\exp(-KL) + (1-\exp(-KL))\cdot\exp(-1/\lambda)\right] \qquad (2)$$

$$I_{Mg}=I^{\infty}_{Mg}\left[\exp(-1/\lambda)+[\exp(-n/\lambda)-\exp(-1/\lambda)]\cdot[1-\exp(-C(L-L_o)^2)]\right] \qquad (3)$$

where L is the exposure value (L)

K is a factor relating oxygen impingement rate to the number of adsorption sites (L^{-1})

n is the average thickness of the islands (ML)

C is a parameter related to the density of nuclei ($Torr^{-2}s^{-2}$)

and L_o is the oxygen exposure at which oxide nuclei first appear (L)

Equations (2) and (3) were fitted to the data of Figure 5(a) using non-linear regression. The solid line in Figure 5(a) shows the line of best fit obtained for the parameters given in Table 1. The value for the escape depth of the electrons, λ, was determined to be about 1.5 monolayers. This value closely matches that estimated using the empirical formulae of Seah and Dench[12] for 45 eV electrons in MgO or $Mg(OH)_2$, viz. 1.6 monolayers for the instrument geometry. Consequently, the parameter estimates provided in Table 1 are deemed to be reasonably accurate. These parameters suggest that the oxidation process of pure magnesium consists of chemisorption followed by oxide nucleation at approximately 0.7 L exposure. This is followed by oxide island growth with coalescence of the islands occurring after the islands have reached an average height of about 4 monolayers. Beyond this stage (~5 L exposure, Figure 5(b)), a diffusion-controlled logarithmic growth of oxide appears to dominate. Work is continuing on this type of analysis for the series of iron-containing alloys. In so doing, it is thought that the exact role that iron plays in the oxidation process of magnesium can be elucidated.

Table 1: Best fit parameters

λ (ML)	K (L^{-1})	n (ML)	C ($Torr^{-2}\,s^{-2}$)	L_o (L)
1.55	1.6	4.2	4.1×10^{11}	0.70

CONCLUSIONS

1. On magnesium alloys containing iron at concentrations ranging from 70 to 700 ppm, the growth rate of the initial oxide is retarded on grains exhibiting bright secondary electron channeling contrast with the retardation effect a clear function of iron concentration. Although this effect is not yet understood, it is the first known example where the presence of a very minor constitiuent is shown to alter the oxide growth rate from the earliest possible stage.

2. Three stages of early oxide growth on pure magnesium have been recognized: a chemisorption stage during doses up to 0.75 L; a rapid oxide nucleation and growth stage which is complete by about 5 L; and a slow growth stage after coalescence of the oxide islands.

FUTURE WORK

This work is continuing in several directions. First, the orientation (or at least the index level) will be determined for crystal planes where the growth rate of the oxide is affected by the presence of an alloying constitiuent. This will be done by preparing thin TEM foils of the specimens already studied and measuring selected area diffraction for the grains studied.

It is particularly important to carry exposures through from 100 L to the megaLangmuir level, understanding the role of substrate orientation, metallic defect density and alloy composition on the structure of the film. During this regime, parabolic growth conditions are likely established. Scanning Auger microscopy is particulary valuable for understanding composition and growth on a microscopic scale. With thicker oxides (> 20 nm), it is hoped that the use of secondary ion mass spectrometry (SIMS) will help to reveal the role of the minor alloying constituent as well as hydrogen in the oxide film. The use of D_2O as a reactant will separate the presence of hydrogen originating in the reactant gas from that of the background.

Finally, the validity of any approach which uses an ion beam to prepare alloy surfaces for reaction needs further study. We plan to compare reaction rates for pure Mg polycrystalline specimens that are prepared by sputter/anneal cycles with those prepared by low ion beam dose alone. For this, a high temperature stage is required for the Auger system. If the differences in reactivity are shown to be low, the approach espoused in this report could be adopted in many other alloy oxidation studies.

REFERENCES

1. J.C. Fuggle, *Surf.Sci.*, **69**, 581 (1977).

2. H. Namba, J. Darville and J.M. Gilles, *Surf.Sci.*, **108**, 446 (1981).

3. B.E. Hayden, E.Schweitzer, R.Kotz and A.M. Bradshaw, *Surf.Sci.*, **111**, 26 (1981).

4. S.A. Flodström and C.W.B. Martinsson, *Surf.Sci.*, **118**, 513 (1982).

5. M.A. Barteau and X.D. Peng, *Mater.Chem.Phys.*, **18**, 425 (1988).

6. S.J. Splinter and N.S. McIntyre, Progress Report 6, SJS-SSW-06, (1991).

7. J.W. Christian, The Theory of Transformations in Metals and Alloys: Part I. Equilibrium and General Kinetic Theory, Permagon Press (1975).

8. P.H. Holloway, *J.Vac.Sci.Tech.*, **18**, 653 (1981).

9. D.F. Mitchell, P.B. Sewell and M. Cohen, *Surf.Sci.*, **61**, 335 (1976) and *Surf.Sci.*, **69**, 310 (1977).

10. P.H. Holloway and J.B. Hudson, *Surf.Sci.*, **45**, 123 (1974) and *Surf.Sci.*, **45**, 141 (1974).

11. C. Palacio, H.J. Mathieu and D. Landolt, *Surf.Sci.*, **182**, 41 (1987) and *Surf.Sci.*, **189/190**, 168 (1987).

12. M.P Seah and W.A. Dench, *Surf.Interface Anal.*, **1**, 1 (1979).

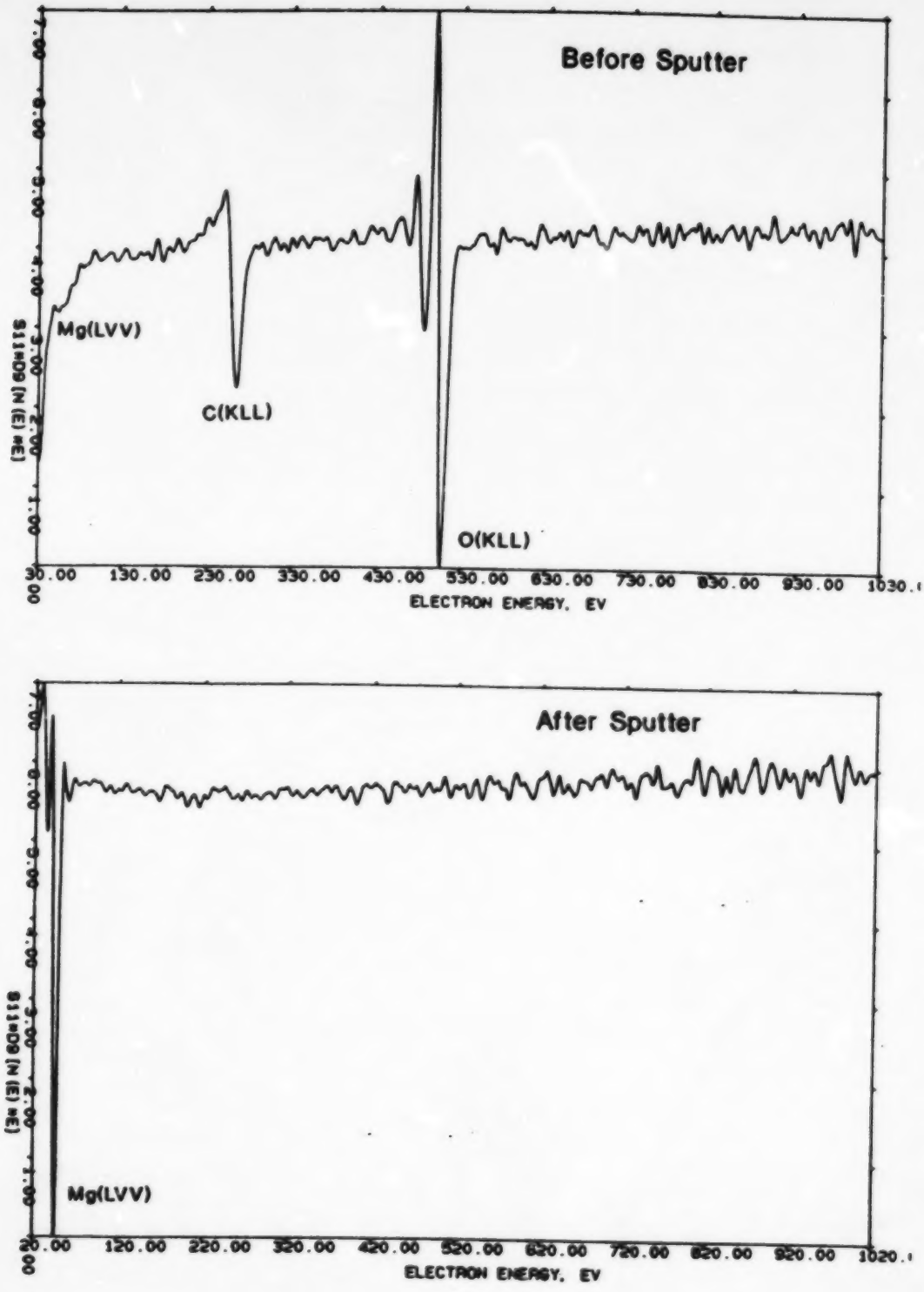

Figure 1: Auger survey spectra of pure magnesium surfaces. The as mounted surface (a) shows contamination by carbon and oxygen. A brief sputter with 3 keV argon ions results in a surface free of contamination, (b).

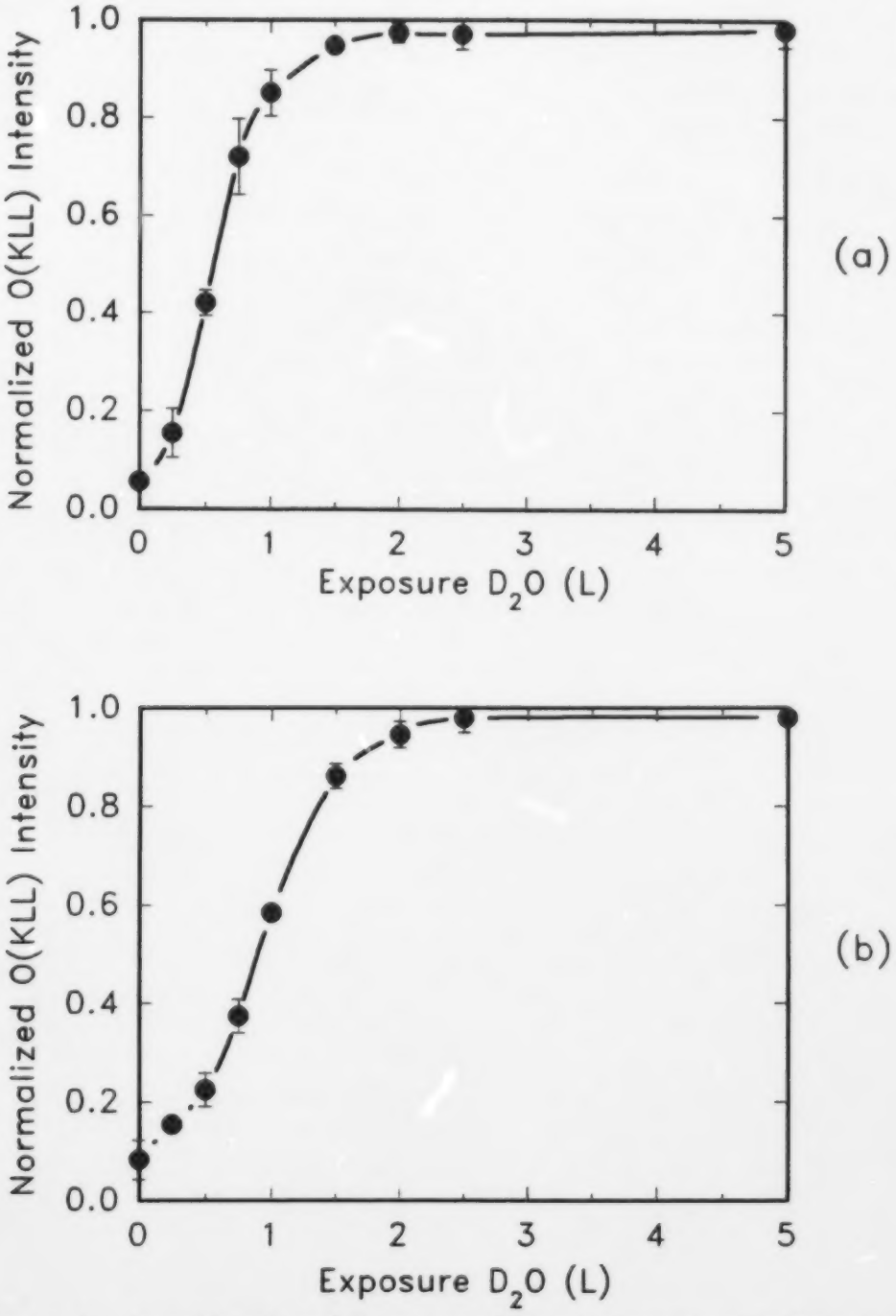

Figure 2: Growth of oxide on grains of pure magnesium exhibiting (a) bright secondary electron channeling contrast and (b) dark contrast. The grains are shown in (c). The growth is monitored as an increase in the O(KLL) Auger signal intensity with D2O exposure.

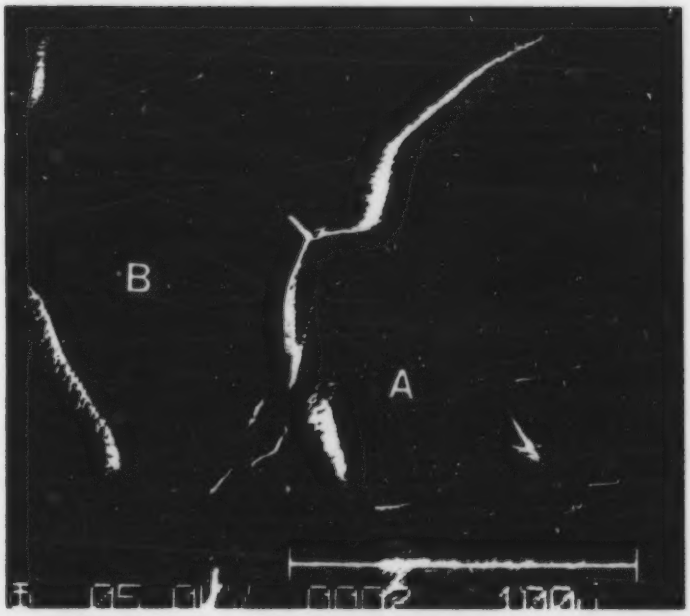

Figure 2(c): Scanning electron micrograph of grains analysed in (a) and (b).

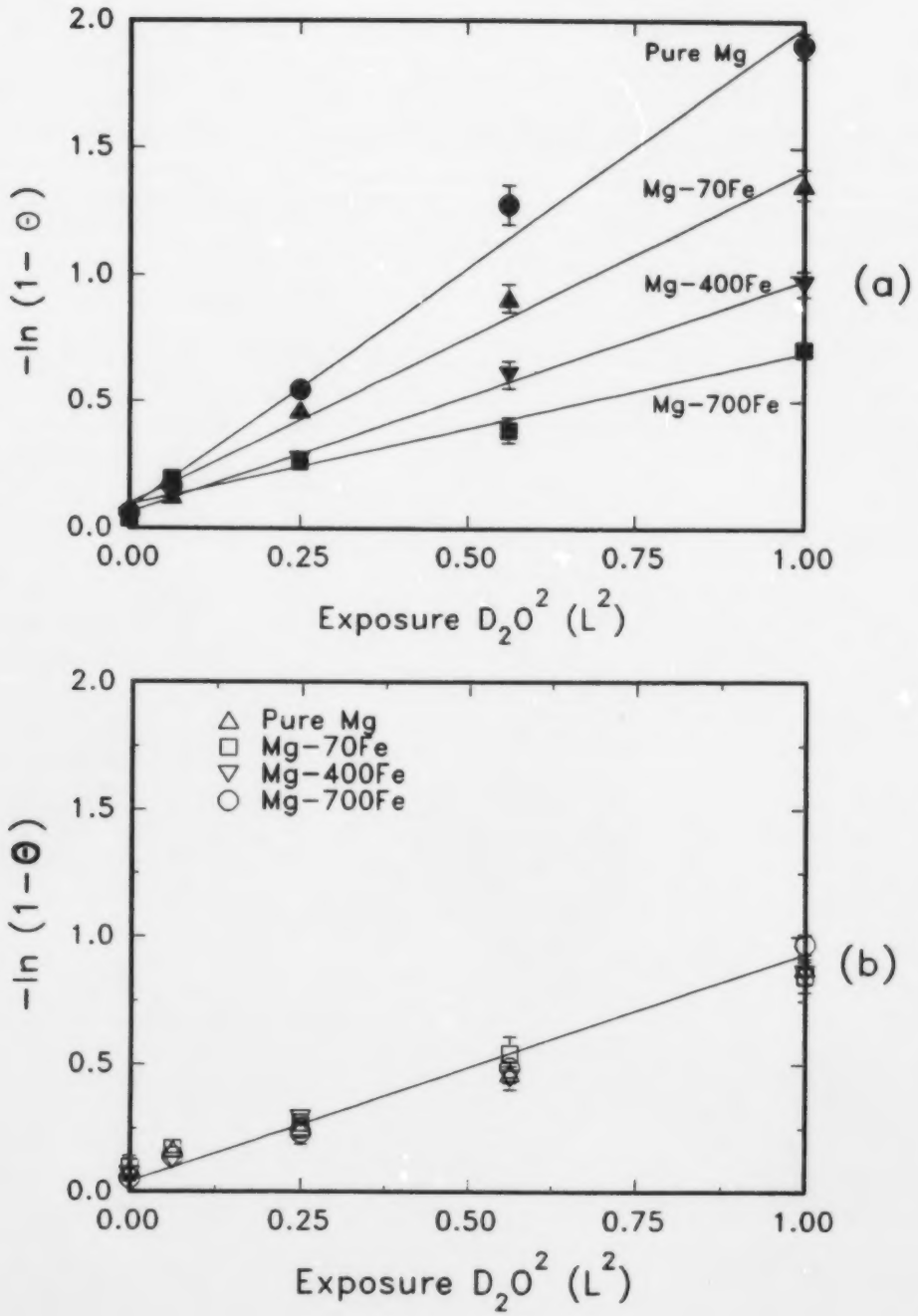

Figure 3: Oxygen uptake on grains exhibiting (a) bright contrast and (b) dark contrast on pure magnesium and magnesium alloyed with 70, 400 and 700 ppm Fe. The data are fitted to a 2-D nucleation and growth model where the magnitude of the slopes represents the rate of oxygen uptake.

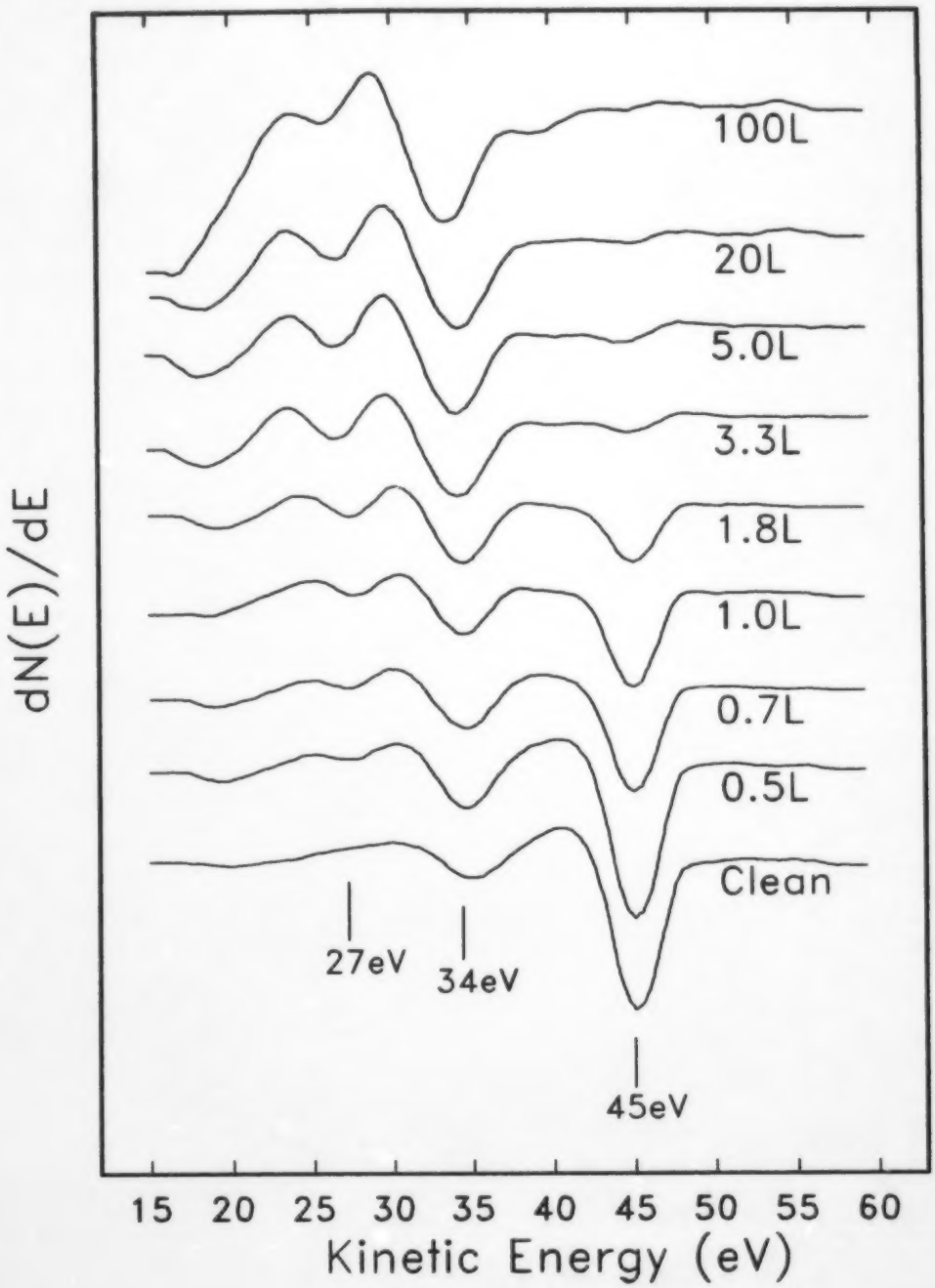

Figure 4: Changes in the low-energy magnesium Auger signal for increasing exposures to D2O on a grain of pure magnesium exhibiting dark secondary electron channeling contrast.

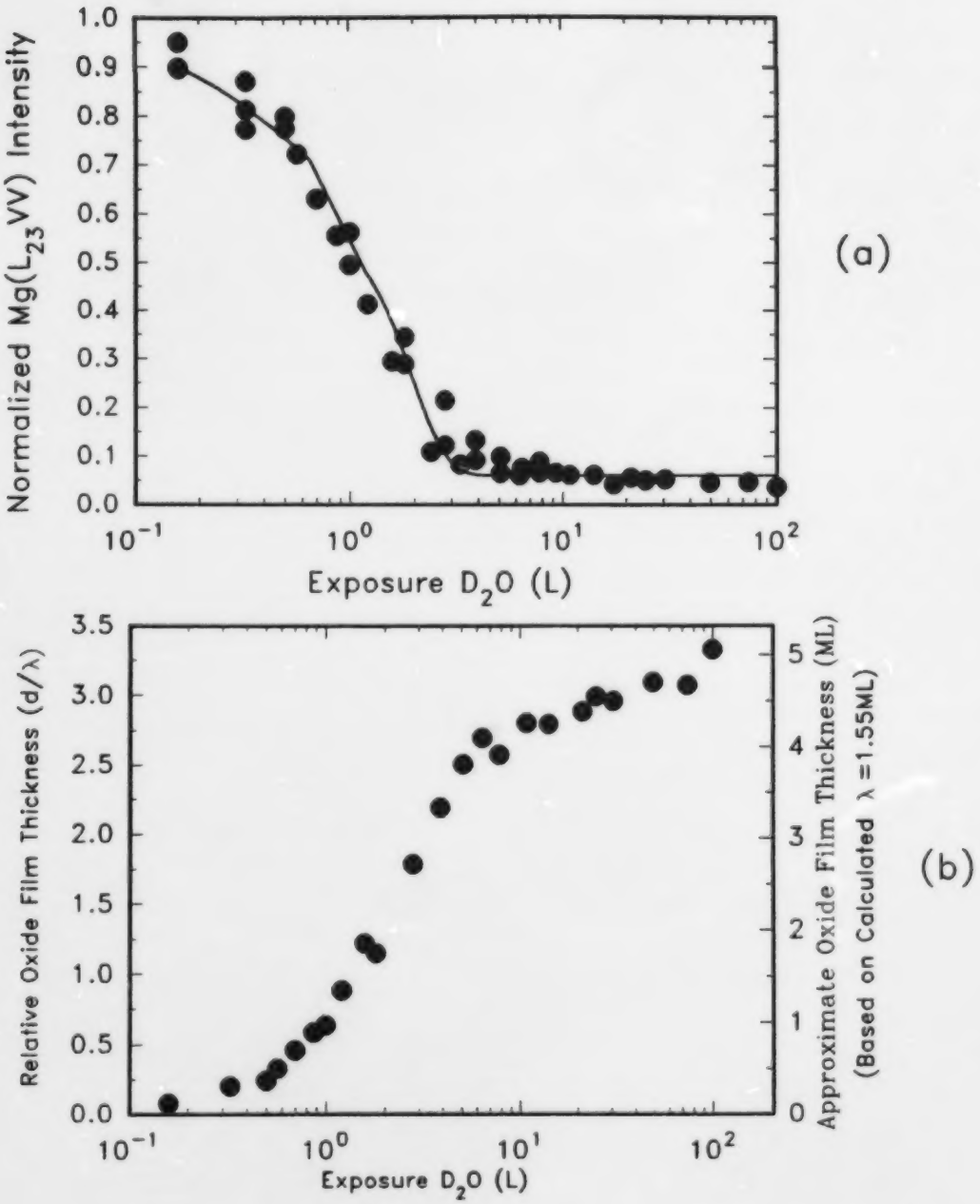

Figure 5: The growth of oxide on a dark grain of pure magnesium. (a) The attenuation of the metallic Mg(LVV) AES signal where the solid line represents the best fit line of equations (2) and (3) with the parameters of Table 1. (b) The relative oxide film thickness obtained from the data of (a) and equation (1). The right hand scale was calculated using the best fit parameter for the escape depth, λ, of the Mg(LVV) electrons.